Hierarchical and operando tomography with x-rays and beyond

Christoph Rau *[a,b,c], Darren Batey [a], Shashi Marathe [a], Leonard Turpin [a], Kudakwashe Jakata [a], Silvia Cipiccia [d], Isabel Antony [a,d], Roberto Volpe [e], Claus-Peter Richter [b], Alessandra Carriero [f], Maud Dumoux [g], Jürgen E. Schneider [h], Erica Dall'Armellina [h], Marc W. Holderied [i], Jan Van den Bulcke [j,k]

[a] Diamond Light Source, Harwell Science and Innovation Campus, Didcot, OX110DE, UK
[b] Northwestern University, 320 E. Superior Street, Chicago, IL 60611-3008, USA
[c] University of Manchester, School of Materials, Grosvenor St., Manchester, M1 7HS, UK
[d] University College London, Department of Medical Physics and Biomedical Engineering, Gower Street, London, UK
[e] Queen Mary University of London, School of Engineering and Materials Science, Mile End Road, London E1 4NS, UK
[f] City College New York, 160 Convent Avenue, ST-403C, New York, NY 10031, USA
[g] Rosalind Franklin Institute, Harwell Science and Innovation Campus, Didcot, OX11 0FA, UK
[h] University of Leeds, Institute of Cardiovascular and Metabolic Medicine, University of Leeds, Leeds, LS2 9JT, UK
[i] University of Bristol, Life Science Building, 24 Tyndall Ave., Bristol, BS8 1TQ, UK
[j] U Gent-Woodlab, Department of Environment, Faculty of Bioscience Engineering, Ghent University, Coupure links 653, 9000 Ghent, Belgium
[k] Centre for X-ray Tomography, Ghent University, 9000 Ghent, Belgium

ABSTRACT

We report about the experimental work related to hierarchical structures at the Diamond I13L beamlines. The I13-2 Imaging and I13-1 Coherence beamlines provide imaging with micro- and nano-resolution. The Diamond II upgrade for the synchrotron source and the OCTOPI upgrade for I13L provide new opportunities for expanding the existing scientific areas in multiscale and *operando* imaging. We describe the scientific research benefitting from the instrumental upgrade. Comparable recording times across all length scales will enable hierarchical *operando* imaging. With the implementation of automated high-throughput data acquisition and analysis, large numbers of samples will be analyzed.

Keywords: Synchrotron, Tomography, Multiscale, Operando, High-Throughput

1. INTRODUCTION

The connection between structures and their function is often determined by features expanding over several orders in length scales. Examples are the study of heart diseases starting from the molecular level to the macroscopic expression of the pathology, failure of materials such as the formation of cracks in battery electrodes, or the evolution of pore networks on ligno-cellulosic biomass during thermochemical treatments. In all cases, various methods are applied to cover the essential features of the system in detail.

For this purpose, currently two independently operating beamlines at I13L address the topic employing a variety of experimental methods. The Diamond OCTOPI flagship upgrade for the I13L beamlines aims to increase throughput and recording speed, closing the gap between methods for data acquisition, achieving *operando* tomography throughout all length scales. Micro-tomography can be performed with an automated sample changer to up to 300 samples per day. The capabilities of the full-field microscope are improved for Zernike-type microscopy and the grating interferometer is developed further. The I13-1 coherence beamline improves constantly the recording speed beyond 10kHz and most recently even 100kHz.

Developments in X-Ray Tomography XV, edited by Bert Müller, Ge Wang, Proc. of SPIE
Vol. 13152, 131521C · © The Authors. Published under a Creative Commons
Attribution CC-BY 3.0 License · doi: 10.1117/12.3033126

2. THE I13L BEAMLINES

Diamond Light Source is a third-generation synchrotron radiation source, operating a significant number of X-ray imaging beamlines in scanning and full-field mode. The electron microscopes, available for physical and life sciences, extend the imaging capabilities to higher resolution. The Diamond I13L beamlines cover the micron- to the nano-length scale 3D-Imaging in the 6-30keV X-ray energy range. They consist of two independent beamlines, operating in real and reciprocal space (see Figure 1)[1,2]. On the I13-2 Imaging beamline tomographic data is recorded within minutes, using in-line phase contrast for micron and full-field microscopy for nano-resolution. The neighbor I13-1 Coherence beamline permits ultimate resolution, using ptychography. The capabilities are completed with grating interferometry (I13-2) [3] and Bragg-CDI/Bragg-Ptychography (I13-1), both combine simultaneous micro- and nano-measuring.

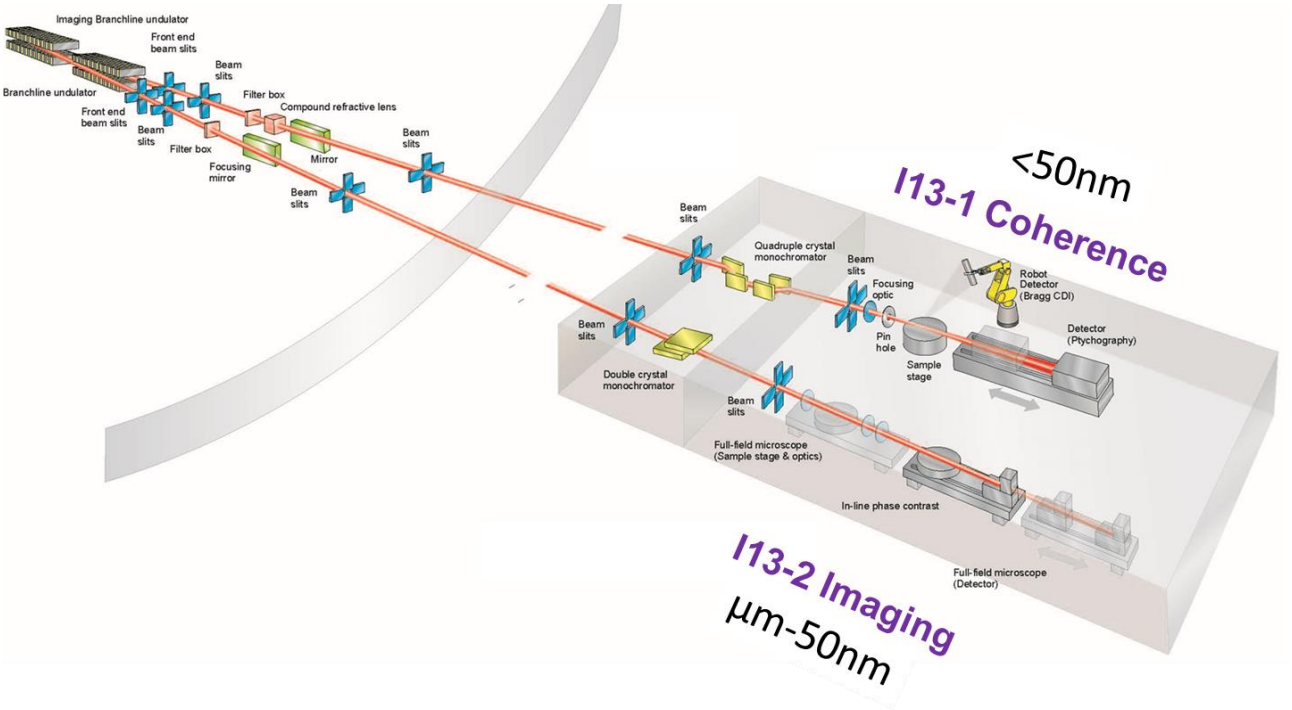

Figure 1. Scheme for the I13L beamlines.

3. CURRENT SCIENCE AND INSTRUMENTATION

3.1 Pyrolysis of Biochar

The synthesis of micro- nano-porous materials from ligno-cellulosic biomass is important for numerous pore-dependent applications such as air or water remediation. For example, biochars (the carbonaceous material resulting from the pyrolysis of biomass) can help reduce the concentration of bacteria and organic pollutants from hospitals wastewaters. Importantly such materials offer a facile and inexpensive route to water remediation in developing countries, where access to clean water is not guaranteed to all. As such, the synthesis of widely accessible sustainable porous materials is essential. Yet, understanding how porosity evolves during the preparation of biochars and correlating particle morphology with the parameters of the thermal process is challenging. The aim of the study is to achieve a better understanding of the underlying principles of the pyrolysis process and to produce a reliable and economical manufacturing scheme for these materials.

The initial study was carried out on the I13-2 Imaging beamline. The experimental setup is shown in Figure 2. The starting material was held in a small capillary and then mounted onto the vertically rotating sample stage of the setup. The capillary was heated under a flow of Argon, see left side picture 2. The heat ramp was set to 10 degrees per minute, peak temperatures between 300 and 600 °C were reached and samples held at peak temperatures for 10 minutes before being cooled down to room temperature. The sample was scanned continuously during the heating and cooling phases. Approximately 58 full scans were taken per run and each scan (~ took about 1 minute to complete. This short duration was key to ensure limited sample movement/change during each scan.

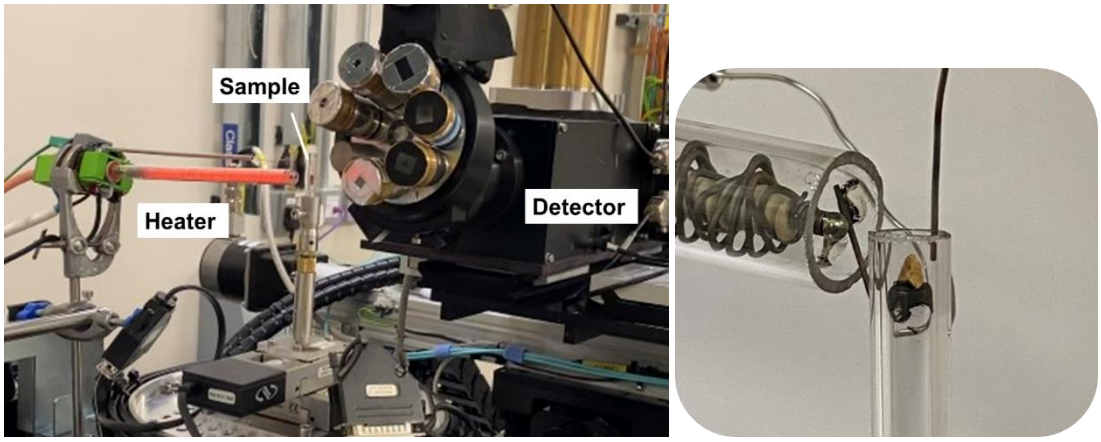

Figure 2. Experimental setup for studying pyrolyze with in-line phase contrast tomography.

The typical cross section of a ~2mm diameter biochar particle is shown in Figure 3, left. Importantly, the pore size and its distribution across the sample does not only depend on the heating protocol but also on the sample preparation (Figure 3 right). For example, it was found that when single particles of walnut shells are washed with deionized water ahead of the heating process, the overall porosity increases significantly, and so does the location of pores towards the center of the particle. This was a key finding, not only for applications such as the afore mentioned water remediation, but also to advance fundamental understanding of pyrolysis of ligno-cellulosic biomass. In highly lignified samples, such as walnut shells, the evolution of particle porosity during the heating process is driven by the ill-understood role of lignin, a highly cross-linked three-dimensional biopolymer present in the vast majority of plant species.

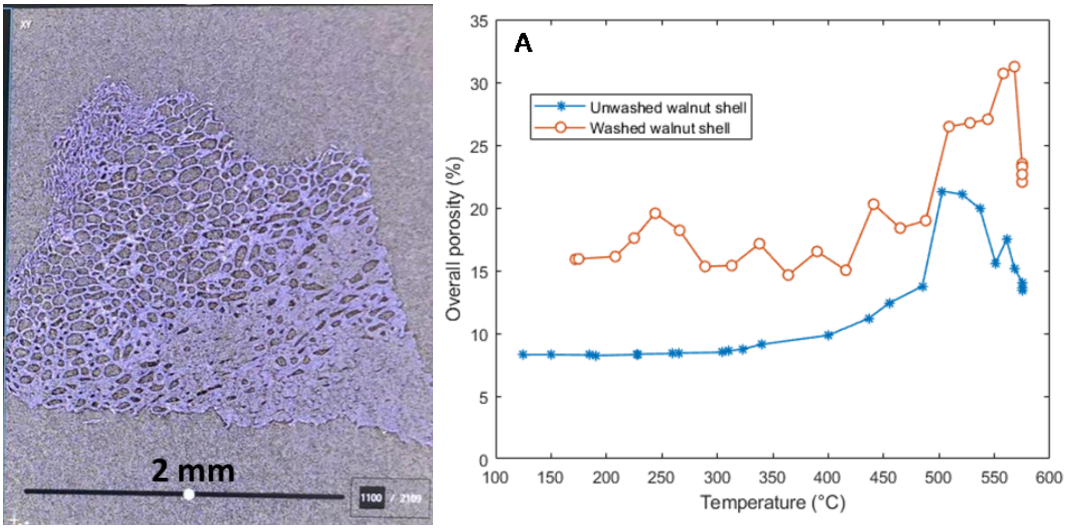

Figure 3. Representative reconstructed slice of a pyrolyzed biochar (left) and influence of sample preparation on pore size distribution (right).

By observing the evolution of the morphological structure of the sample, in *operando*, we found that during heating, the presence of alkali and alkali-earth metals (K, Ca) traces in the shell nucleates the formation of more thermally stable carbon structures (such as graphitic domains) originating from lignin. Pre-washing the material is known for removing significant amounts of metals, thereby resulting in a more homogeneous distribution of pores and the pore diameters through the particle volume during pyrolysis [4]. The filtering properties of biochars depend on their specific surface. While the pore size and their distribution can be measured with micro-tomography (hundreds of nanometers), the full resolution of the surface requires significantly higher spatial resolution (tens of nanometers). For this purpose, several other methods need to be employed. We did meanwhile some demonstration studies on similar materials using full-field X-ray microscopy (TXM), electron microscopy and most recently ptychography (see Figure 4).

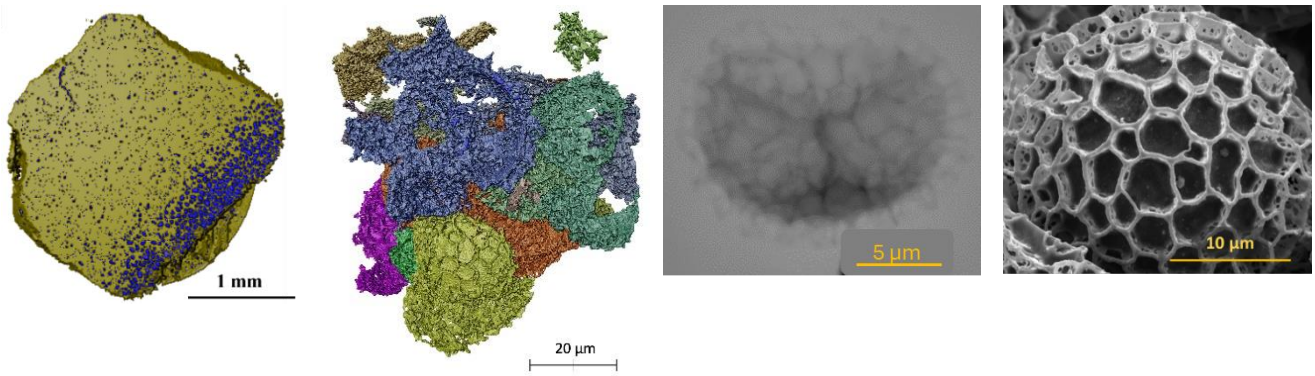

Figure 4. Left to right: Comparison measurements micro-tomography, full-field microscopy (TXM), ptychography and e^- microscopy.

3.2 Multiscale structure of moth wings

The study of natural structures provides much innovation for engineering and advancements in our daily lives. At the beamline we studied the structure of insect eyes, giving an understanding about the underlying optics and the consequences for the species [5]. The brilliant colors of some species, for examples butterflies, are explained by their micro- and nano-structures and may be explored for modern paints. Most recently, we studied the micro- and nano- structure of moth wings for their acoustic properties (see Figure 5). Indeed, their specific features make moths undetectable for their predators, namely bats. By simulating and analyzing the acoustics in the following, the gained understanding serves for developing sound damping materials.
By micro-tomographic studies it was shown that the intricate scale layers on moth wings form a metamaterial ultrasound absorber with a peak sound intensity absorption of about 72% at 78kHz [6,7]. At higher spatial resolution, the study of porosity and the fine composition of the scales provide the completed picture of the acoustic properties.

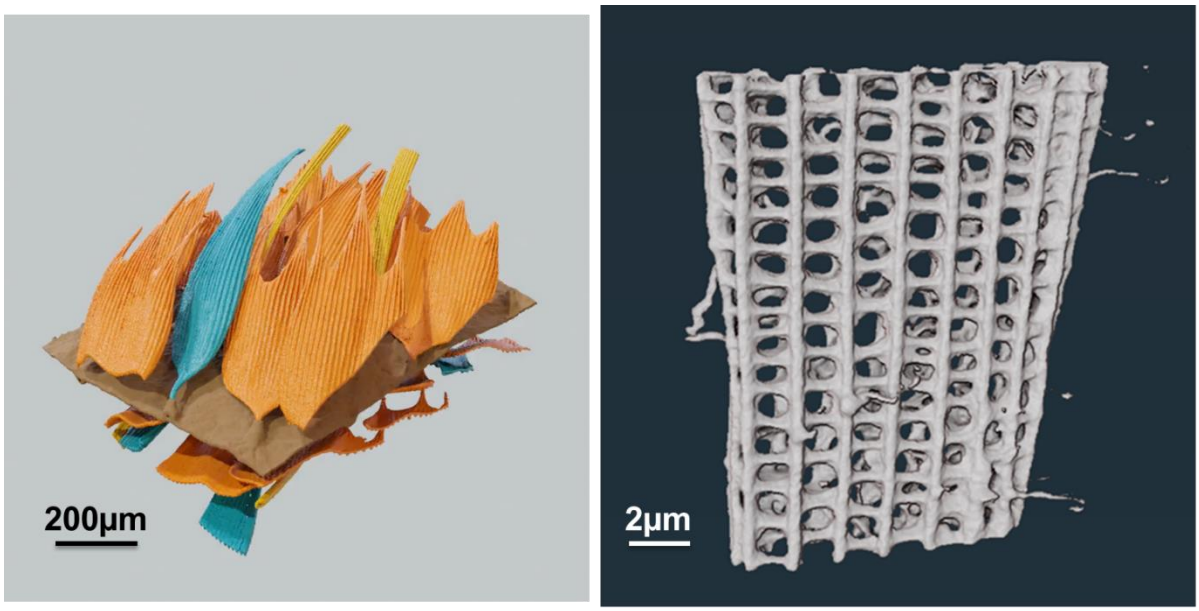

Figure 5. Volume rendering of micro-tomographic (left) and ptychographic (right) data of a moth (Lepidoptera) wing. Colors on the left panel distinguish different types of scales (brown: ‘spoon’, blue: ‘spade’, yellow: ‘hair’).

3.3 Study of heart diseases with X-rays and beyond

The aim of the study is to connect the macroscopic expression of heart diseases to their microscopic origins at the molecular level. The approach includes a variety of techniques beyond the use of X-rays. Several classes of heart diseases are targeted for the study, for example hypertrophic cardiomyopathy (HCM), which can lead to sudden cardiac death (SCD). Features of this disease can be identified with magnetic resonance imaging (MRI) at a late stage of the disease and a deeper understanding for the molecular origins are required for enabling appropriate medication early on.
For our studies it has been demonstrated that diffusion tensor MRI is valid, and the measurements were complemented with micro-tomography data on the imaging branch [8,9]. Finer section of the hearts will be investigated with the TXM, ptychography and ultimately with electron microscopy (see scheme Figure 6)[10]. Essential for this type of study are sample preparation, embedding and measurement protocols, and potentially cryo-cooling of the samples.

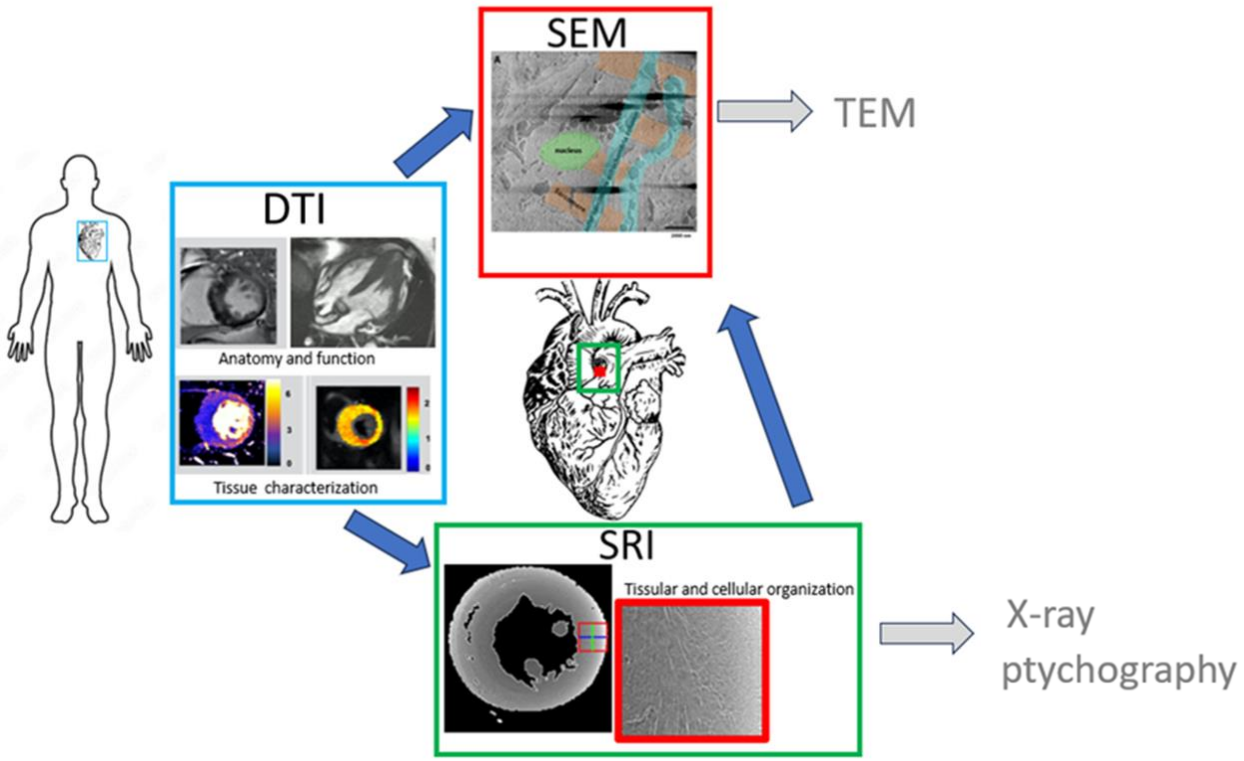

Figure 6: Schematic representation for the multi-scale imaging with X-ray complementing methods to investigate heart diseases, including diffusion tensor magnetic resonance imaging (DTI), synchrotron radiation imaging (SRI) and scanning/transmission electron microscopy (SEM/TEM).

3.4 Studying cellular and sub-cellular porosity for bone fragility, cell mechano-sensing and calcium homeostasis

Bone is strong and tough and adapts its shape in response to the applied loads. The highly organized hierarchical structure of bone together with its tissue (re)modeling dynamics and microdamage mechanisms, confer bone the ability to withstand loads without deformations and fractures, and to adapt to its mechanical environment. Aging and disease disrupt bone hierarchical structure, have altered bone (re)modelling and microdamage mechanisms, thus increasing bone vulnerability to deformities and fractures. Bone (re)modelling is orchestrated by osteocyte cells that are embedded in the matrix within a cave (lacuna) and connected to each other by dendrites running in the matrix through small canals called canaliculi. Osteocytes are all connected to each other and their system forms the osteocyte lacunar canalicular network (LCN). Between the osteocytes and the extracellular matrix there is some interstitial fluid that flows in the LCN as the bone is loaded. Because of the LCN, osteocytes are able to sense the mechanical stimulus on bone and recruit osteoclast cells to resorb bone and osteoblast cells to deposit new bone through (re)modelling. While remodeling refers to the ability of bone to resorb and deposit new bone sequentially in the same bone location, bone modeling instead refers to the ability of bone to shape or reshape by the independent (uncoupled anatomically or temporally) action of osteoblast and osteoclasts.
We here aim to study the LCN porosity in healthy and osteogenesis imperfecta (OI or *brittle bone disease*) bone using synchrotron radiation-based transmission X-ray microscopy so to elucidate the effect of their architecture on controlling bone quality, and particularly fragility, cell mechano-sensing and calcium homeostasis. We compared healthy and osteogenesis imperfecta affected mouse long bones to study their cell populations. For this purpose, we used the full-field microscope (TXM) at I13-2 with a resolution of about 80nm at 9 or 12 keV photon energy (see Figure 7). The contrast can be modulated with Zernike phase rings in positive and negative mode. The exposure times are about 100ms when using energy bandwidth limited pink-beam with the multilayer monochromator [11,12].

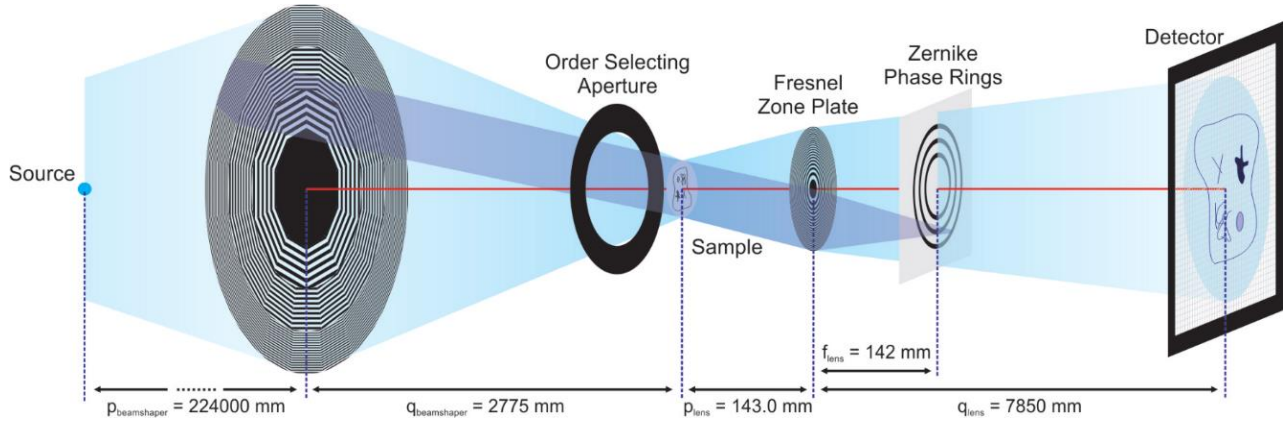

Figure 7. Scheme for the full-field microscope (TXM) at I13-2 Imaging.

The Zernike method enhances significantly the contrast in samples and can be even inverted (negative Zernike phase contrast) as demonstrated in Figure 8, top rows. When applying the method to the investigation in bones, in the positive mode lacunae and canaliculi can be detected which become even more visible in the negative Zernike phase contrast mode. With the negative ZPC, cells and dendrites become visible within their lacunae and canaliculi, respectively. The method is currently improved further to suppress image artifacts, permitting easy segmentation and rendering of the data for quantitative analysis.

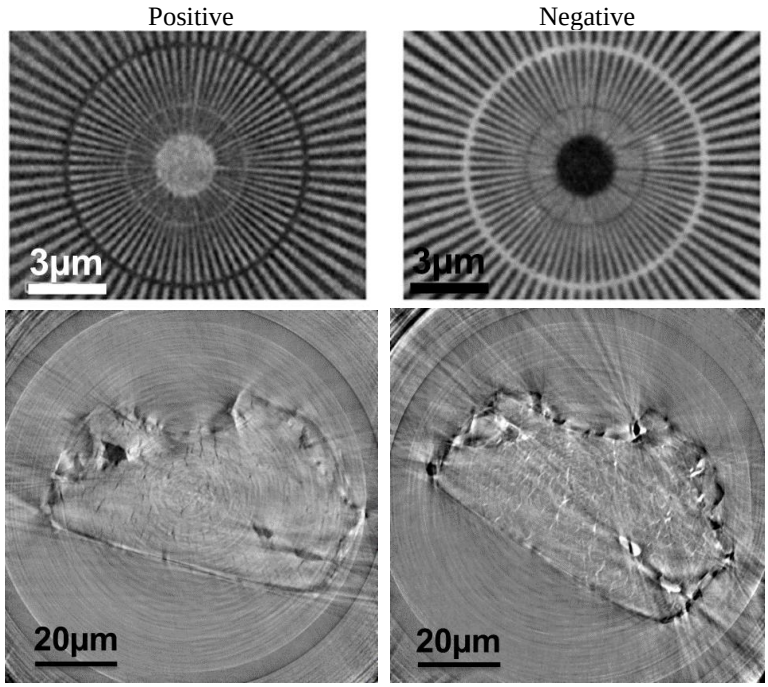

Figure 8: Top: Demonstration of Zernike phase contrast microscopy method for enhancing and even inverting contrast. Bottom: Measurement of femoral bone cellular porosity with Zernike phase contrast (left positive, right negative).

4. UPGRADES: DIAMOND II AND OCTOPI

Starting end 2027, Diamond II is the major upgrade of the electron storage ring, increasing the electron energy from 3 to 3.5GeV and reducing the emittance by about two orders of magnitude. Beamlines are upgraded before, during and after that period and OCTOPI '*Operando Computed TOmographic & Ptychographic Imaging'* is the flagship upgrade for the I13L beamlines [13]. The impact of the Diamond II machine upgrade for the beamline performance are expected to be the reduction in recording times by a factor of about 100 for high resolution coherent imaging (ptychography and Bragg-CDI) and 10 times for imaging on the micron scale. For the I13-1 Coherence beamline, the improvement is mostly related to the lower emittance/increased brilliance of the source. For the I13-2 Imaging beamline a new insertion device will mainly increase the photon flux and enable accessing higher X-ray photon energies. The gap in recording speed between the spatial resolutions will be reduced (see Figure 9), enabling multi-scale operando imaging under comparable conditions. The instrumentation will be adapted to the new possibilities with engineered end-stations, namely for ptychography, Bragg-CDI and full-field microscopy.

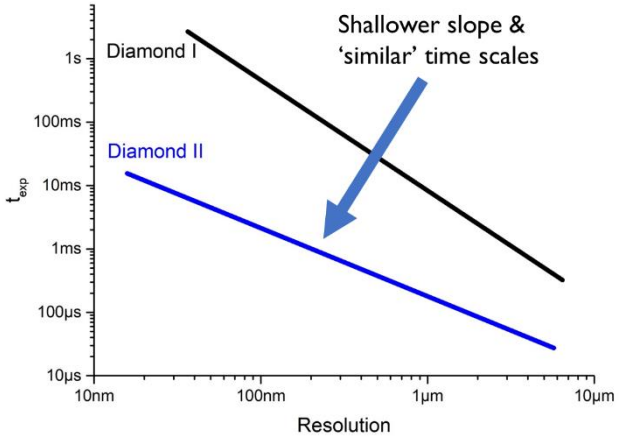

Figure 9: The Diamond II upgrade will provide compatible exposure times across all length scales.

4.1 Scientific Impact: Study of Crystallization and other cases

The Diamond II upgrade will enhance the science already explored at the beamline and described in some examples above. The study of phenomena and processes, previously unachievable, will become accessible. This is the case for the crystallization processes during the mixing of a solution with an anti-solvent (see Figure 10)[13]. Currently micro-crystallization can be studied in a flow-reactor, but the upgrade will permit the observation at highest spatial resolution of earliest and smallest nucleation cluster. With highest temporal resolution nucleation kinetics can be observed.

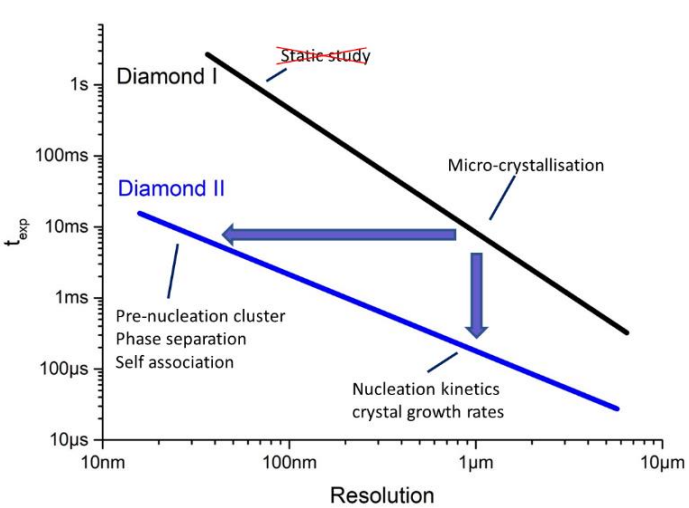

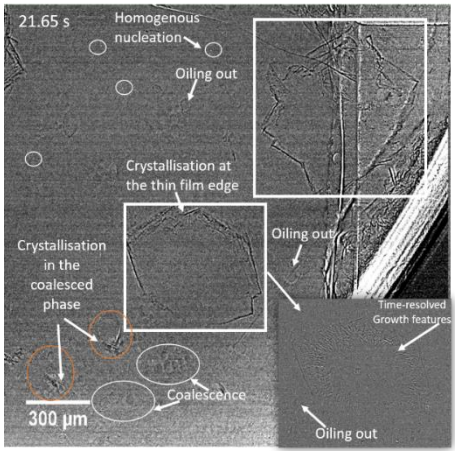

Figure 10: Science impact of Diamond II upgrade at the example of crystallization processes [1].

4.2 High throughput recording

An automated sample changer, consisting of a robotic arm, a gripper mechanism and a telescope camera for automated sample alignment has been installed with the capacity of running up to 300 samples per day. The device is now routinely used for static samples and the applications are numerous. The systematic cataloging of insects (collaboration A. Goswami, Natural History Museum, London) to understand the large biodiversity of insect and the adaption of their physiognomy to their habitat is one example of handling fragile and sometimes unique specimen. Experiments can also be caried out in zoom-in mode, selecting the areas of interest with a higher magnification objective lens of the detector (see Figure 11, experiment J. Van den Bulcke). This capability is frequently exploited, requiring some manual intervention for selecting the relevant areas. The investigation of wood is a typical example for a hierarchical study upon a large number of samples. Beamtime can be scheduled more flexible and each experimental session can be shorter. This benefits for long term studies as for example the research project for the avoidance of complications in pregnancies by case studies on placenta. Samples are collected over an extended period of time and about half a dozen sessions have been run for the work (Gowsihan Poologasundarampillai, University of Birmingham).

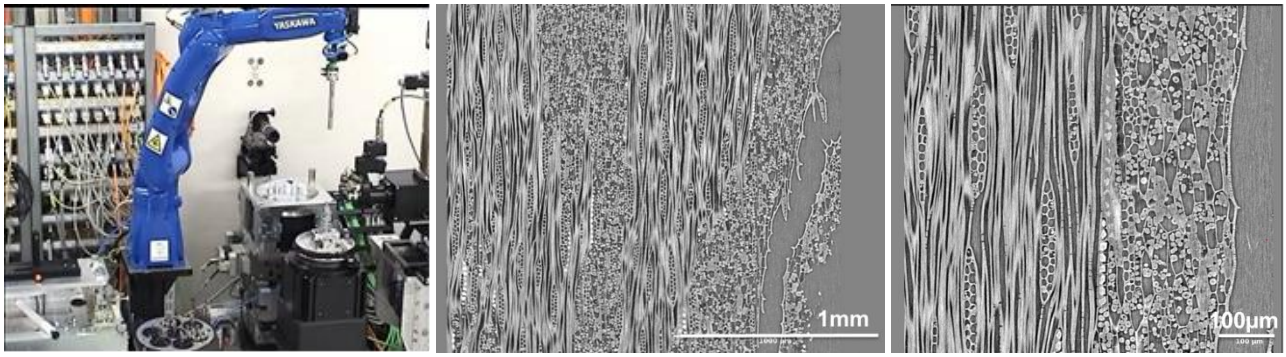

Figure 11: Left: robotic sample changer, middle and right: reconstructed data of African wood species (*Afzelia bella*), scanned at different magnifications and at similar sagittal sections (courtesy J. Van den Bulcke).

The diameter for samples of 5mm is currently increased to 8mm using a new gripper mechanism. The setup has the potential for any remote/mail-in and commercial use and may be developed upon request by the community.

4.3 Fast recording at highest resolution

For the I13-2 Imaging beamline fast imaging is enabled using the polychromatic radiation of the source either by filtering the beam by a combination of X-ray filters and the deflection of the X-ray mirror or by using a multilayer monochromator. Recording times are typically in the msec and occasionally in the µsec range. The flux is to be increased for smaller samples and the TXM with collimating optics recently installed. The I13-1 Coherence beamline has systematically improved the recording speed, much related to the increased triggering speed of the recording chain and detector system. The increase to 9kHz has been demonstrated [14] and most recently a pilot experiment with the latest generation of Dectris detectors at a triggering rate of over 100kHz has been achieved. An area of 800µm^2 /sec can be scanned with currently 175nm resolution and will largely benefit from the upgrade in coherent flux with Diamond II.

5. SUMMARY

The I13L beamlines I13-1 Coherence and I13-2 Imaging complement each other for multi-scale and operando imaging for numerous scientific applications. The Diamond II upgrade will close the gap in recording times across the length scales and enable multi-scale operando imaging and tomography. Automated sample scanning is frequently used for micro-tomography using a robotic arm. With manual intervention, ‘zooming’ studies are enabled for a large number of samples. At the highest resolutions, with ptychography, the rapid recording chain with up to 100kHz detector triggering will largely benefit from the Diamond II upgrade.

Additional information about the instrumental details of the upgrade can be found in [13], and the underlying principles for the methods namely in-line phase contrast imaging [15], full-field microscopy including Zernike phase contrast [16-19] and automated data acquisition [20-23].

ACKNOWLEDGEMENTS

Kaz Wanelik, Huw Shorthouse, Tim Ardern and all support teams at Diamond Light Source are greatly acknowledged for their work at the beamlines. Sylvia Britto and Konstantin Ignatyev from I18 provided help with their furnace for the pyrolysis experiments. The work is supported by the Diamond-Manchester collaboration. The contributions to the experiments by the different research teams, namely Luis Salinas-Farran, Maryanne Mosonik, (R. Volpe, Queen Mary, London), G. Broad, B. Price, O. Kippax-Chui (A. Goswami, NHM, London), Asier Munoz, Maialen Ugarteburu (A. Carriero CCNY, New York), M. Farzi, I. Teh (J. Schneider, Leeds), Louis Verschuren, Sofie Dierickx, Matthieu Boone (J. Van den Bulcke, UGCT-UGent), are greatly appreciated. The present publication is dedicated to Ljubo Zaja, who contributed substantially to the engineering work at the beamline and lately to the automated sample changer project.

REFERENCES

[1] C. Rau, U. Wagner, Z. Pesic and A. De Fanis, "Coherent imaging at the Diamond beamline I13," Physica Status Solidi a-Applications and Materials Science, 208(11) (2011), 2522-2525.
[2] C. Rau, C., "Imaging with Coherent Synchrotron Radiation: X-ray Imaging and Coherence Beamline (I13) at Diamond Light Source," Synchrotron Radiation News, 30(5) (2017),19-25.
[3] S. Marathe, R. F. Ziesche, G. Das, S. L. M. Schröder, E. Baird, C. Rau, 'High-speed grating interferometry', Proceedings of SPIE 2021, 11840, (2021) pp. 11840 10.1117/12.2598481.
[4] L. Salinas-Farran, M.C. Mosonik, R. Jervis, S. Marathe, C. Rau, R. Volpe, 'Tracked evolution of single biochar particle's morphology during pyrolysis in operando x-ray micro-computed tomography'. *Biochar* **6**, 86 (2024), 1-14, https://doi.org/10.1007/s42773-024-00374-7R.
[5] G. J. Taylor, P. Tichit, M. D. Schmidt, A. J. Bodey, C. Rau, E. Baird, 'Bumblebee visual allometry results in locally improved resolution and globally improved sensitivity', Elife 8 (2017), 1-32, DOI: 10.7554/eLife.40613.
[6] H. Mendoza Nava, M. W. Holderied, A. Pirrera, R. J. Groh, 'Buckling-induced sound production in the aeroelastic tymbals of Yponomeuta', Proceedings of The National Academy Of Sciences 121 (2024), DOI: 10.1073/pnas.2313549121.
[7] T. R. Neil, Z. Shen, D. Robert, B. W. Drinkwater, M. W. Holderied, 'Moth wings are acoustic metamaterials', Proceedings Of The National Academy Of Sciences 47 (2020), 31134–31141, DOI: 10.1073/pnas.2014531117.
[8] M. Farzi, S. Coveney, M. Afzali, M.-C. Zdora, C. A. Lygate, C. Rau, A. F. Frangi, E. Dall'Armellina, I. Teh, J. E. Schneider, 'Measuring cardiomyocyte cellular characteristics in cardiac hypertrophy using diffusion-weighted MRI', Magnetic Resonance in Medicine 4 (2023), 2144-2157, DOI: 10.1002/mrm.29775.
[9] I. Teh, D. McClymont, M.-C. Zdora, H. J. Whittington, V. Davidoiu, J. Lee, C. A. Lygate, C. Rau, I. Zanette, J. E. Schneider, 'Validation of diffusion tensor MRI measurements of cardiac microstructure with structure tensor synchrotron radiation imaging', Journal of Cardiovascular Magnetic Resonance 19 (2017), 1-14, DOI: 10.1186/s12968-017-0342-x.
[10] M. Dumoux, T. Glen, J. LR Smith, E. ML Ho, L. MA Perdigão, A. Pennington, S. Klumpe, N. BY Yee, D. A. Farmer, P. YA Lai, W. Bowles, R. Kelley, J. M Plitzko, L. Wu, M. Basham, D. K Clare, C A. Siebert, M. C Darrow, J. H Naismith, M. Grange, 'Cryo-plasma FIB/SEM volume imaging of biological specimens', eLife (2019), 1-33, 8:e40613.12:e83623.
[11] M. Storm, F. Döring, S. Marathe, S. Cipiccia, C. David, C. Rau, 'Optimizing the energy bandwidth for transmission full-field X-ray microscopy experiments', Journal of Synchrotron Radiation 29 (2021), 138-147, 10.1107/S1600577521011206.
[12] M. Storm, F. Döring, S. Marathe, C. David, C. Rau, 'The Diamond I13 full-field transmission X-ray microscope: a Zernike phase-contrast setup for material sciences', Powder Diffraction 425 (2020),1 – 7, DOI: 10.1017/S0885715620000238.

[13] C. Rau, S. Marathe, A. J. Bodey, M. Storm, D. Batey, S. Cipiccia, P. Li, R. F. Ziesche, M. Al-Hada, Sven L. M. Schröder, G. Das, A. Goswami, 'Operando and high-throughput micro and nano-tomography', Proc. SPIE 11840, (2021),118401E-18401E-9, 10.1117/12.2598470.
[14] D. Batey, C. Rau, S. Cipiccia. 'High-speed X-ray ptychographic tomography', Sci Rep 12, 7846 (2022), 1-6, https://doi.org/10.1038/s4198-022-11292-8.
[15] P. Spanne, C. Raven, I. Snigireva, A. Snigirev, 'In-line holography and phase-contrast microtomography with high energy x-rays', Phys. Med. Biol. 44 (1999), 741-749.
[16] M. Stampanoni, R. Mokso, F. Marone, J. Vila-Comamala, S. Gorelick, P. Trtik, K. Jefimovs, C. David, 'Phase-contrast tomography at the nanoscale using hard x rays', *Physical Review B* **81** (2010),140105-1-140105-4.
[17] K. Jefimovs, J. Vila-Comamala, M. Stampanoni, B. Kaulich, C. David, 'Beam-shaping condenser lenses for full-field transmission X-ray microscopy', Journal of Synchrotron Radiation 15 (2008), 106-108.
[18] M. Storm, S. Cipiccia, S. Marathe, V.S.C. Kuppili, F. Doring, C. David, C. Rau, 'The Diamond I13-2 Transmission X-ray Microscope: Current Status and Future Developments', Microscopy and Microanalysis, 24(S2) (2018), 216-217.
[19] J. Vila-Comamala, J. Bosgra, D. S. Eastwood, U. Wagner, A.J. Bodey, M. Garcia-Fernandez, C. David, C. Rau, 'Transmission X-ray Microscopy at Diamond-Manchester I13 Imaging Branchline', AIP Conference Proceedings, 1696 (2016), 020036-1-020036-4.
[20] F. De Carlo, X. Xiao, B. Tieman, 'X-ray tomography system, automation, and remote access at beamline 2-BM of the Advanced Photon Source', *Proc. SPIE,* **6318** (2006), 63180K-1-63180K-13.
[21] K. Mader, F. Marone, C. Hintermüller, G. Mikuljan, A. Isenegger, M. Stampanoni, 'High-throughput full-automatic synchrotron-based tomographic microscopy. J Synchrotron Radiation (2011), 117-124, DOI: 10.1107/S0909049510047370.
[22] T. Baumbach, private communication.
[23] J. Albers, M. Nikolova, A. Svetlove, N. Darif, M.J. Lawson, T.R. Schneider, Y. Schwab, G. Bourenkov, E. Duke, 'High Throughput Tomography (HiTT) on EMBL beamline P14 on PETRA III', J Synchrotron Radiation (2024), 186-194, DOI: 10.1107/s160057752300944x.